PHYSICAL REVIEW A VOLUME 55, NUMBER 2 FEBRUARY 1997

Electron scattering by Ca atoms and photodetachment of Ca^- ions: An *R*-matrix study

Jianmin Yuan[1,2] and L. Fritsche[1]

[1]*Institut für Theoretische Physik B, Technische Universität Clausthal, D-38678 Clausthal-Zellerfeld, Federal Republic of Germany*

[2]*Department of Applied Physics, National University of Defense Technology, Changsha 410073, People's Republic of China*

(Received 25 July 1996; revised manuscript received 17 September 1996)

We have performed close-coupling calculations on electron scattering by Ca atoms and on photodetachment of Ca^- ions by using a six-state (^1S- ^3P- ^3D- ^1D- ^1P- ^1P) *R*-matrix method. We predict a strong interaction between $(4s^{2}\,{}^1S+\epsilon d)^2D$ and $(4s4p\,{}^3P+\epsilon p)^2D$ channels that gives rise to two relatively broad resonance peaks in the *d*-wave cross section. In addition, one obtains a strong and a weak peak in the total scattering cross section. Our calculations on the photodetachment cross section of Ca^- ions yield results that are in good qualitative agreement with the experimental data by allowing for the opening of a detachment channel connected to the excited state $4s4p\,{}^3P$. [S1050-2947(97)01401-7]

PACS number(s): 34.80.Bm, 34.80.Dp, 32.80.Fb

I. INTRODUCTION

Negative alkaline-earth ions have been extensively studied during the past few years [1–10]. These studies were concerned with bound states [1–4] as well as with scattering states [5–8]. Only two articles deal with the photodetachment of negative Ca^- ions [9,10]. The growing interest in the study of electron interaction with alkaline-earth atoms has been stimulated by the experimental discovery that these closed-shell atoms form stable negative ions. Pegg *et al.* [1] were the first to discover the stability of Ca^-. Hence, in all the subsequently published work on negative alkaline-earth atoms this ion has always been included as a standard.

Except for earlier close-coupling calculations by Fabrikant [11], all of the more recent theoretical studies on electron scattering by Ca atoms are essentially one-channel calculations, though correlation effects are taken into account in a variety of ways. The close-coupling results of Fabrikant are marred by the fact that the atomic wave function is generated in a model potential that gives rise to some inaccuracy that can hardly be assessed. In the work of Amusia *et al.* [12] and in later studies by Gribakin *et al.* [7], both based on solving the Dyson equation, an effective potential is derived that governs the motion of the projectile electron within the atom and contains carefully incorporated correlation effects. However, it cannot directly be recognized how the coupling of the various channels affects the collision cross section. The work of Yuan and Zhang [5] draws on a static exchange approximation where correlation effects are accounted for by using an averaged correlation potential familiar from density-functional theory. In a recent calculation by Semytkowski and Sienkiewicz [8], a relativistic polarized orbital method was used to generate the polarization potential. All of these one-channel calculations [5–8] gave similar results, i.e., they agree in the essential features of the predicted cross sections.

There is one experimental study by Romanyuk *et al.* [13] on the low-energy regime of electron collision with Ca atoms. These experiments refer to impact energies of a few eV and have recently been refined [14]. Within the range of 0–10 eV, the authors find a strong peak around 0.7 eV as a main feature of the total cross section and a small nearby peak at 1.7 eV. The position of the two peaks has recently been found to be shifted up by about 0.4 eV as a result of experimental refinements. All the theoretical studies mentioned above agree reasonably well in the prediction of the first peak, but they fail in explaining the occurrence of the second small peak. Experiments by Johnston *et al.* [15] on electron transmission in Ca vapor within an energy regime of 0–4 eV provide less directly, information on the low-energy cross section of Ca atoms. Two resonances are found within this energy range. The results can be explained in terms of strongly mixed $4s^23d\,{}^2D$ and $4s4p^{2}\,{}^2D$ states of the Ca^- ion, which proves to be in accord with their configuration-interaction calculation.

As for the photodetachment of Ca^- ions, only two calculations have so far been carried out. One is due to Gribakin *et al.* [9] and the other one to Fischer and Hansen [10]. The work of the former authors was based on the Dyson equation, while the latter draws on a multiconfiguration Hartree-Fock scheme. Both calculations, however, refer to photodetachment cross sections below 0.2 Ry. Hence they can only in part be compared to the measurements of Heinicke *et al.* [16], whose photon energies extend considerably higher up. These experiments date relatively far back. As the properties of the negative ion were clear at that time, the authors were not able to give an unambiguous explanation of their experimental results.

In the present article we report a six-state (^1S, ^3P, ^3D, ^1D, ^1P, and ^1P) close-coupling calculation based on the *R*-matrix algorithm of Berrington *et al.* [17]. As will be evidenced by our results, there is a strong interaction between the shape resonant channel $(4s^{2}\,{}^1S+\epsilon d)^2D$ and the excitation channel $(4s4p\,{}^3P+\epsilon p)^2D$ which is responsible for the additional weak structure in the total cross section of electron scattering. Furthermore, the general features of the photodetachment cross section as measured by Heinicke *et al.* [16] can be explained fairly well, if one allows for the opening of a detachment channel ^2P that is connected to an excited $4s4p\,{}^3P$ state.

II. METHOD OF CALCULATION

The *R*-matrix method for electron-atom and photon-atom interactions has been discussed in great detail by Burke *et al.*

© 1997 The American Physical Society

TABLE I. Parameters of the Slater-type basis functions.

Orbitals	C_{jnl}	I_{jnl}	ξ_{jnl}
5s	−.54691	1	25.48182
	.00038	2	1.00000
	.04462	2	.78772
	.04017	3	.74615
	.44399	3	13.33072
	58.84367	4	8.95486
	−.62595	4	2.27416
	.17142	5	2.18162
	−.00035	5	.45902
	−35.76805	5	6.47786
6s	−8.17160	1	19.97310
	−.27835	1	32.50886
	−21.12326	2	17.23940
	26.19336	2	8.40361
	136.64572	3	7.46907
	−178.73075	3	3.96008
	125.38981	3	2.95632
	−90.43788	4	3.10847
	3.47253	4	1.63082
	−.53497	4	1.06899
	.03586	4	.74974
4p	−5.99628	2	11.93492
	−10.78447	2	8.05561
	10.00783	3	1.45560
	−9.42999	3	1.41968
	−.02857	4	.78363
	13.07262	4	4.54967
5p	113.17938	2	6.64369
	−107.26783	2	6.55201
	−.10465	3	1.39197
	.06686	3	.77051
	−.00004	4	.26677
	−3.31572	4	3.84949
	−.00022	5	.43101
	.01328	5	1.53292
6p	−912.38655	2	9.12943
	1129.34405	2	16.24803
	1572.08914	3	7.39661
	−65.90903	3	3.63176
	5.39315	3	2.31770
	−.15663	3	1.50250
3d	16.17439	3	5.21826
	.62689	3	.86934
	−.13045	4	1.06762
	−.13068	4	1.10783
	6.61293	5	3.95258
	11.05389	5	5.18334
	.00002	6	.55407
	−.00002	6	.56221
4d	7.04736	3	5.81731
	.42628	3	.95906
	−.09616	4	.88798
	−.09972	4	1.18356
	7.78032	5	5.09555
	2.22618	5	5.14651
	.01447	6	1.26286
	−.00003	6	.48676
5d	3.54344	3	4.84963
	.05814	3	.93013
	−.01527	4	.57552
	.03195	4	1.13505
	−3.12069	5	3.99648
	6.09399	5	4.03649
	.00159	6	.86441
	.00000	6	.27130
6d	23.79912	3	5.41866
	1.10750	3	.87237
	−.83305	4	1.05910
	.13869	4	1.12616
	9.15256	5	3.98919
	25.22434	5	5.53250
	−.00062	6	.59944
	.00086	6	.62214
4f	2.02724	4	1.62358
	.00000	4	.25314
	−.48491	4	1.52121
	.00446	4	.76441
	−.21390	4	1.35822

[18]. The present calculations have been carried out by using the R-matrix package of Berrington *et al.* [17]. In an R-matrix calculation, the wave function of the $N+1$ electron system is given the form

$$\Psi_k(X_1\cdots X_{N+1})=\sum_{ij} c_{ijk}\Phi_i(X_1\cdots X_N\hat{\mathbf{r}}_{N+1}\sigma_{N+1})\times u_{ij}(r_{N+1})+\sum_j d_{jk}\phi_j(X_1\cdots X_{N+1}), \tag{1}$$

where the basis functions under the first sum refer to the continuum, those under the second sum to bound states. Bound-state orbitals are cast as linear combinations of Slater-type orbitals

$$P_{nl}=\sum_j C_{jnl}r^{I_{jnl}}\exp(-\xi_{jnl}r), \tag{2}$$

The pertinent parameters and coefficients C_{jnl} for 1s, 2s, 2p, 3s, 3p, and 4s orbitals are identical with those of the Hartree-Fock orbitals given by Clementi and Roetti [19] for the Ca ground-state. In addition to these Hartree-Fock orbitals, another set of ten virtual orbitals (5s,6s,4p,5p,6p,3d,4d,5d,6d,4f) is used in constructing the wave function. The number of Slater-type orbitals necessary to sufficiently approximate these orbitals P_{nl} according to Eq. (2) increases as the number of spherical nodes of P_{nl} becomes larger. A 4f orbital can satisfactorily be represented by five Slater-type basis functions, a 6s orbital, however, requires 11 basis functions. The parameters in Eq. (2) are optimized independently by using the proven CIV3 computer code [20] in fitting the energy levels of atomic Ca. The

TABLE II. Calculated energies of the first six lowest states of atomic Ca.

State	Energy (Ry)
$(4s^2)^1S$	$-1353.565\,21$
$(4s4p)^3P$	$-1353.432\,58$
$(4s3d)^3D$	$-1353.346\,06$
$(4s3d)^1D$	$-1353.341\,23$
$(4s4p+3d4p)^1P$	$-1353.339\,00$
$(4s5p+3d4p)^1P$	$-1353.228\,24$

results are compiled in Table I. The atomic energy levels that are used as a reference and the calculated energies are listed in Table II. The R-matrix boundary was chosen to be $RA=50$ a.u. In forming the $(N+1)$-electron configurations in Eq. (1), all excitations of the two $4s$-valence electrons into any of the virtual orbitals are allowed for only excluding the possibility of having more than one electron in a $4f$ orbital. As for the construction of the continuum states, we use 6 to 15 angular-momentum orbitals, depending on the energy of the projectile electron, each of these orbitals being expressed as a linear combination of 20 numerical basis functions.

III. RESULTS AND DISCUSSION

A. Electron scattering by Ca atoms

The low-energy electron-scattering cross section of Ca atoms is distinct by a low-lying d-wave-shape resonance around 1.0 eV that was predicted at different positions by various authors [5–8,12]. Some calculations seemed to indicate that there was an additional p-wave-shape resonance near zero energy [12,21]. However, the existence of a stable negative ion Ca^- that contains an extra electron bound in a $4p$ orbital excludes the possibility of a p-wave-shape resonance in the continuum. Some recent calculations [5–7] gave a Ramsauer-Townsend minimum structure in the cross section below the d-wave resonance peak. The only direct measurement of the total cross section of Ca was carried out by Romanyuk *et al.* [13,14]. These authors obtained a main peak around 0.7 eV and a minor structure at 1.7 eV. They recently refined their measurement and found the dominant peak moved to higher energy at 1.2 eV [14]. By using an electron transmission technique, Johnston *et al.* [15] observed a relatively broad resonance centered at 1.1±0.15 eV and a sharp resonance at 2.8±0.15 eV. They interpreted these structures as caused by configuration interaction between the core excited resonance state $4s4p^{2}\,{}^{2}D$ and the shape resonance state $4s^{2}3d\,{}^{2}D$. In our earlier one-channel calculations [5], the shape resonance state $4s^{2}3d\,{}^{2}D$ was predicted to show up at 1.75 eV close to the excitation threshold of the $4s4p\,{}^3P$ state. For this reason, one expects a strong interaction between these two states. This is, in fact, substantiated by the present calculations that the following results refer to.

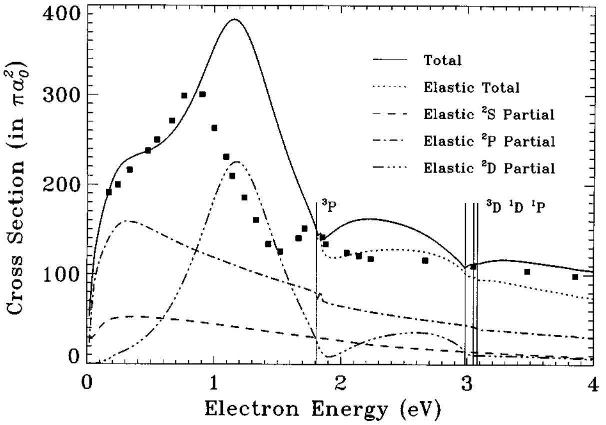

FIG. 1. Total, elastic total, and elastic partial cross sections for electron scattering by Ca atoms. The filled squares refer to the experimental values given in Ref. [13]. The calculated thresholds are indicated by vertical lines.

The dependence of the total cross section of Ca atoms on the impact energy is shown in Fig. 1 together with the respective partial cross sections and the experimental results of Romanyuk *et al.* [13]. The most conspicuous feature consists in two broad peaks of the elastic ${}^2D$ partial-wave cross section at 1.2 and 2.6 eV, respectively. Furthermore, there is a characteristic peak at 1.16 eV and a smaller one at 2.2 eV in the energy dependence of the total cross section. The behavior of the ${}^2D$ partial cross section is indicative of the interaction between the two channels $(4s^{2}\,{}^{1}S+\epsilon d)^2D$ and $(4s4p\,{}^3P+\epsilon p)^2D$. If there are no perturbations from other channels, the core excitation resonance usually appears near the excitation threshold and displays a relatively sharp structure. This contrasts with the present case, where one does not find any resonant structures near the $4s4p\,{}^3P$ excitation threshold (about 1.8 eV), but rather two well-separated broad peaks around 1.2 and 2.6 eV. The positions agree reasonably well with those predicted by Johnston *et al.* [15] who also calculated the width of the two peaks and obtained fairly small values, in particular 0.08 eV for the second peak. Our calculation yields a considerably larger width. As for the first peak of the ${}^2D$ partial-wave cross section, we find that its width is considerably reduced compared to that found in early one-channel calculations [5]. Moreover, its position is shifted from 1.75 down to 1.2 eV. These changes can be attributed mainly to the interaction of the shape resonance state with the core excitation state. A mixture of the core

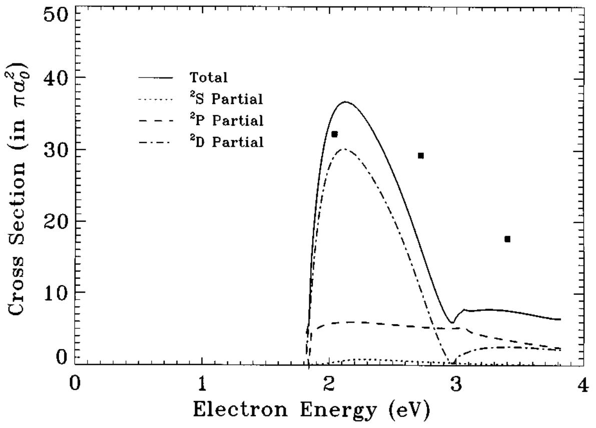

FIG. 2. Cross section for electron-impact excitation of the $\mathrm{Ca}(^3P)$ state. The filled square refers to the calculated result of Ref. [11].

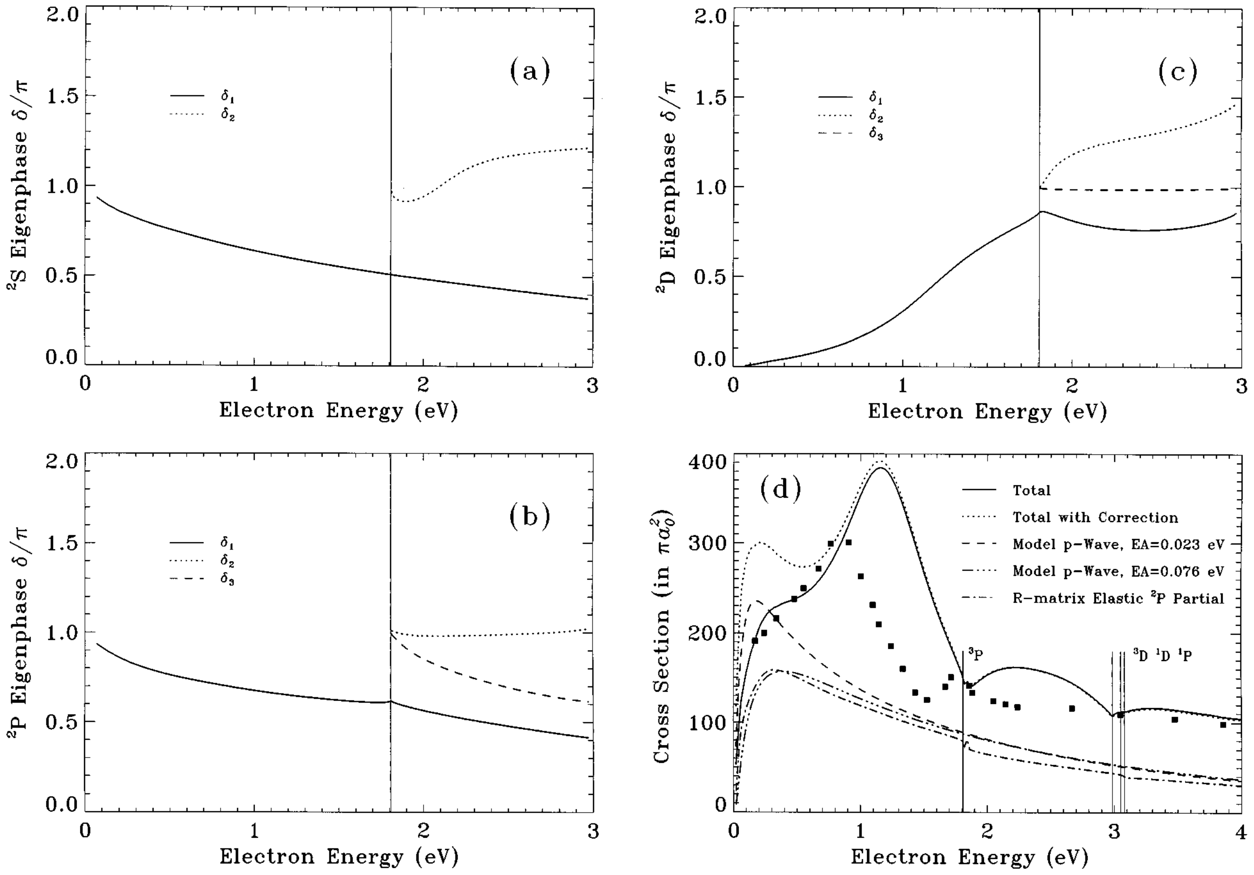

FIG. 3. Energy dependence of the eigenphases of the first three symmetries and the correction to the total cross section by regarding the measured electron affinity: (a) the eigenphases of ^2S symmetry, (b) the eigenphases of ^2P symmetry, (c) the eigenphases of ^2D symmetry, and (d) total cross section after inclusion of a correction that allows for the difference bwtween the calculated electron affinity and experimental electron affinity. The filled squares in (d) refer to the experimental data of Ref. [13]. The threshold energy referring to the Ca(^3P) excited state is indicated by the vertical line.

excitation state with the shape resonance state will certainly reduce the lifetime of the former, which is consistent with the obtained broadening of the second structure. As already stated by Johnston *et al.* in reference to the effect of this channel interaction, it is not clear anymore whether the first peak can still be characterized as relating to a shape resonance and the second one to a core excitation. It should be noted that the ^2S and ^2P partial cross sections do not change as much as those referring to the ^2D partial wave if one compares it to the one-channel calculation [5]. In comparing our results with the earlier experimental total cross section of Romanyuk *et al.* [13,14], one should bear in mind that the relevant structures of the energy dependence have to be shifted up by about 0.4 eV according to their more recent experiment. However, the new results are given only in relative units of the cross section for which reason we have included the earlier results in Fig. 1. Taking these data with the appropriate energy shift as the best presently available reference, we find that the calculated positions of the large and small peaks are in good agreement with the observations. As regards calculations by other authors on this problem, there are two results by Amusia *et al.* [12] that have been already mentioned above and by Gribakin *et al.* [7] who deal, however, with the momentum-transfer cross section only. As for Amusia *et al.*, these authors arrived at values for the position and magnitude of the main d-wave peak that agree closely with ours.

The total cross section that refers to the first excited state $4s4p\,^3P$ is shown in Fig. 2, where we have also included a few partial cross sections and the theoretical results of Fab-

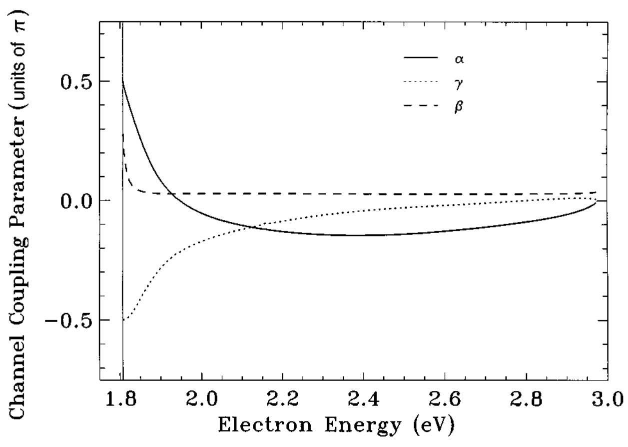

FIG. 4. Energy dependence of the Euler angles referring to the transformation matrix that interconnects the ionization channels $(4s^2\,^1S+\epsilon d)^2D$, $(4s4p\,^3P+\epsilon p)^2D$, and $(4s4p\,^3P+\epsilon f)^2D$, and the eigenchannels.

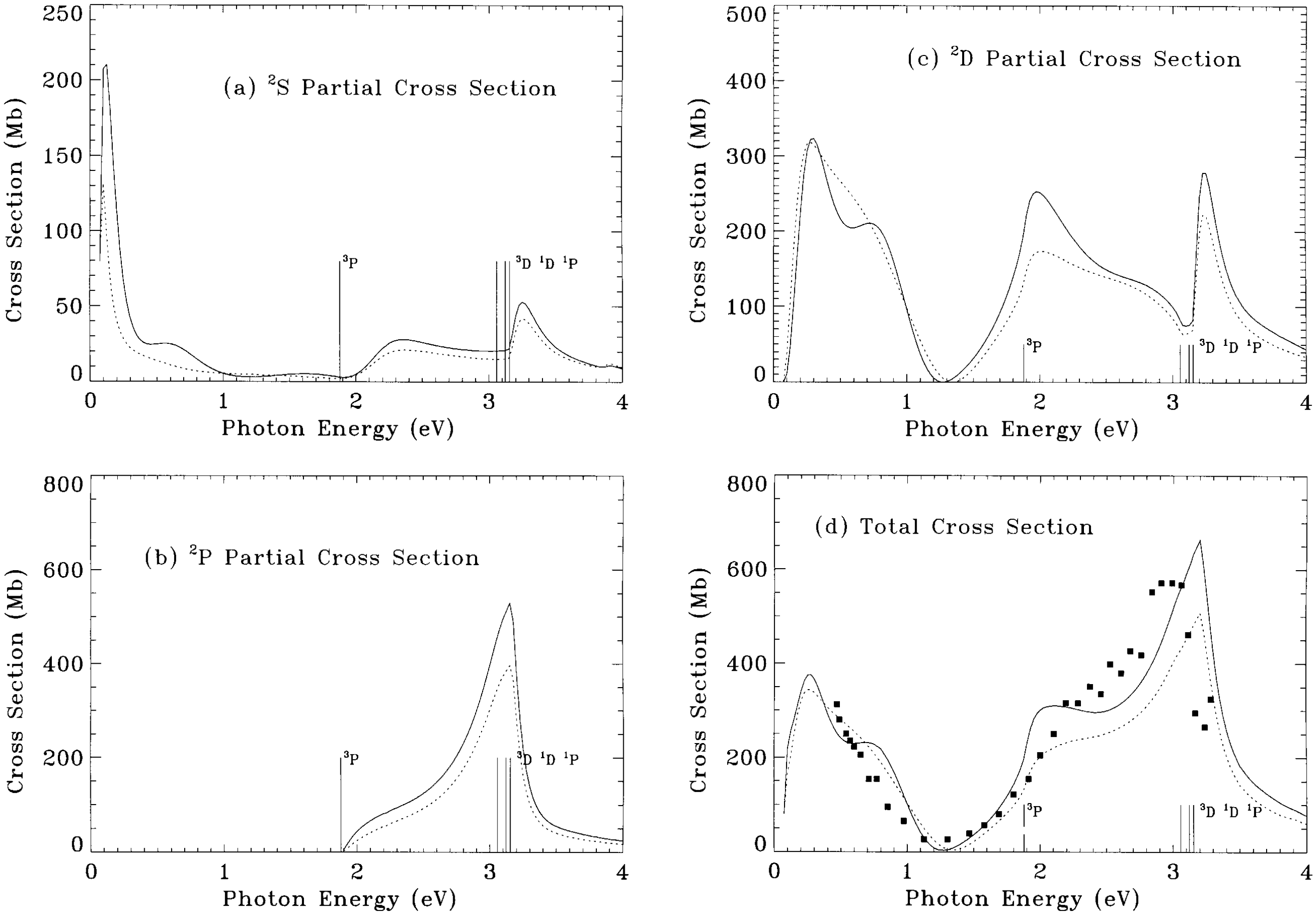

FIG. 5. Total and partial cross sections for photodetachment of the Ca$^-$ ion: (a) ^2S partial cross section, (b) ^2P partial cross section, (c) ^2D partial cross section, and (d) total cross section. Solid lines refer to the length form, dotted lines to the velocity form. The experimental result from Ref. [16] is indicated by the filled squares in (d). Vertical lines depict calculated excitation thresholds.

rikant [11]. The near threshold values of the two calculations are close to each other, but our cross section drops off faster than that of Fabrikant as the impact energy increases. The strong interaction between the two channels $(4s^2{}^1S+\epsilon d)^2D$ and $(4s4p^3P+\epsilon p)^2D$ and the resonance of ^2D symmetry is obviously reflected in the dominance of the ^2D partial cross section.

Figure 3 shows the dependence of the eigenphases of states with ^2S, ^2P, and ^2D symmetry on the collision energy. Obviously, there are two distinct upward curve portions that refer to the ^2D symmetry and reflect the presence of the two resonant states. In fact, the very low-energy ^2P phase shift is closely related to the electron affinity (EA) of the negative Ca$^-$ ions [3,5,22]. In the calculation of Kim and Greene [3], the binding energy of the extra electron was estimated from the p-wave phase shift by using the so-called generalized quantum-defect method [3,23]. In our earlier model calculation [5], the p-wave phase shift was also used to obtain an estimate of the electron affinity. In his study of the decaying of negative ions in an electric field [22], Fabrikant found very small sensitivity of the p-wave phase shift to the value of the binding energy and predicted an electron affinity of 0.021 eV for Ca atoms very close to the most recent experimental data [24]. From the point of view of generalized quantum-defect theory, since the quantum defect changes continuously as one crosses zero energy, the near-zero-energy p-wave phase shift and the corresponding partial cross section are largely determined by the position of the near-zero bound state of the negative ion (if the binding occurs) and the polarizability of the neutral target, regardless of the detailed form of the interaction between the projectile and the target atom.

The above discussion suggests a simply feasible minor correction to the total cross section which Fig. 1 refers to. This correction can be done by using our earlier model potential method where we introduce an adjustable scaling factor that is given two values such that the model potential yields two binding energies, one at 0.076 eV, close to our R-matrix value, and the other one at 0.023 eV close to the most recent experimental value obtained on the electron affinity of Ca [24]. The correction to our R-matrix total cross section is then given by the difference between the corresponding p-wave partial cross sections of these two binding energies. The results are plotted in Fig. 3(d). Obviously, the model potential p-wave partial cross section associated with an electron affinity of 0.076 eV is very close to our R-matrix result at low scattering energy. The correction becomes considerable only at low energies. Its effect consists merely in rising the shoulder of the total cross section below the main peak. Otherwise, it causes hardly any change to the cross section above the main peak.

In order to demonstrate the coupling of the three ionization channels $(4s^{2\,1}S+\epsilon d)^2D$, $(4s4p\,^3P+\epsilon p)^2D$, and $(4s4p\,^3P+\epsilon f)^2D$, we introduce the transformation matrix between the ionization channels and the eigenchannels, written in terms of the associated three Euler angles,

$$\begin{bmatrix} \cos\alpha\cos\beta\cos\gamma-\sin\alpha\sin\gamma & \sin\alpha\cos\beta\cos\gamma+\cos\alpha\sin\gamma & -\sin\beta\cos\gamma \\ -\cos\alpha\cos\beta\sin\gamma-\sin\alpha\cos\gamma & -\sin\alpha\cos\beta\sin\gamma+\cos\alpha\cos\gamma & \sin\beta\sin\gamma \\ \cos\alpha\sin\beta & \sin\alpha\sin\beta & \cos\beta \end{bmatrix}.$$

The energy dependence of the three Euler angles is shown in Fig. 4. The interaction of the two channels is connected with the off-diagonal elements of the matrix, which are known to vary smoothly with energy.

B. Photodetachment of Ca$^-$ ions

An early experiment on the photodetachment of Ca$^-$ is due to Heinicke *et al.* [16]. However, at that time the existence of a stable negative Ca$^-$ ion was not known yet and hence the interpretation of the experiment lacked conclusiveness. More recent experiments by Hanstorp *et al.* [25] are concerned with the photodetachment of metastable excited Ca$^-$ ions. These authors were able to correlate the results of Heinicke *et al.* with the existence of a stable Ca$^-$ state. As this point may now be considered clarified, we shall use the results of Heinicke *et al.* as a basic reference.

As for the theory of photodetachment with stable Ca$^-$ ions there are two studies by Gribakin *et al.* [9] and by Fischer and Hansen [10]. Gribakin *et al.* treated the bound state of the absorbed electron by solving the Dyson equation, thereby including correlation effects. However, the free electron is only described at a Hartree-Fock level. By contrast, Fischer and Hansen use a multiconfiguration Hartree-Fock scheme to incorporate correlation effects into both initial and final states. The results of Gribakin *et al.* and Fischer and Hansen refer to an energy range up to 0.2 Ry. To provide a complete understanding of the experiments it appeared indispensable to us to extend the calculations further up to higher energies even beyond the opening of the first target excitation channel to cover the full experimental range of photon energies.

We use a configuration-interaction wave function to describe the ground-state and the excited state of the target. The radial part of the wave function is constructed by using analytic Slater-type basis functions which are, however, less suited to describe the rather diffuse loosely bound negative ion states. Furthermore, the first six orbitals $(1s,2s,2p,3s,3p,4s)$ are chosen to agree with the Hartree-Fock orbitals of the neutral atom. As for the bound orbital of the negative ion that is involved in the photodetachment process, the above level of accuracy is insufficient. We therefore generate this orbital by using the algorithm ITER [17] within the R-matrix computer code. This amounts to adding 20 numerical basis functions for each angular momentum and extending the wave function beyond the R-matrix boundary. The calculation yields $-1353.570\,74$ Ry for the ground-state energy of the Ca$^-$ ion. If one subtracts this from the target ground-state energy, one obtains an electron affinity of 0.005 52 Ry, which is very close to the results calculated by other authors [2,3]. This indicates that the valence correlation has been included adequately in our calculation. On the other hand, if one would use only the analytic orbitals within the CIV3 computer code, one would obtain a total energy of the Ca$^-$ ion of $-1353.566\,04$ Ry, which agrees less favorably with high-quality calculations. Notwithstanding the comparability of the above affinity energy to results of equivalent calculations that only allow valence correlation as the present study, it is by a factor of 3 larger than the experimental value that has recently been confirmed to be 0.0018 Ry [24]. The origin of this discrepancy may be seen in the omission of core-core and core-valence correlations and in the neglect of relativistic effects [2,26–28].

The results of the present calculation on the total photodetachment cross section are shown in Fig. 5 along with the experimental results of Heinicke *et al.*. The latter data were originally given in arbitrary units. We have scaled them appropriately to alleviate a comparison with our results. Obviously the main features of the experiment are fairly well described by our calculation. As one can see from the partial cross sections that Figs. 5(a)–5(c) refer to, the second peak observed around 3 eV is definitely connected to the ^2P partial cross section. The latter can only play a role once the channel that relates to the excitation of the $4s4p\,^3P$ state has been opened. There is also a contribution of the excitation channels connected to ^2S and ^2D symmetry, but it is less significant compared to the case of ^2P symmetry. Below the first excitation threshold, one is only dealing with the photodetachment channels $(4s^{2\,1}S+\epsilon s)^2S$ and $(4s^{2\,1}S+\epsilon d)^2D$ that structure the ^2S and ^2D partial cross sections. The physics mirrored by these data is the same as that discussed by Fischer and Hansen in their s-wave and d-wave analysis [10].

In comparing our results to those of the latter authors we find good agreement only in the position of the Cooper minimum, but otherwise the photodetachment cross sections differ sizably in magnitude, particularly around the first peak near the threshold. Also, the agreement between the length and velocity form of our results is not as good as in Fischer and Hansen's work. The main difference between our calculation and theirs resides in the description of the target states. They use a numerical multiconfiguration Hartree-Fock scheme to obtain a ground-state energy for the target of $-1353.570\,04$ Ry, which is by 0.004 83 Ry lower than ours.

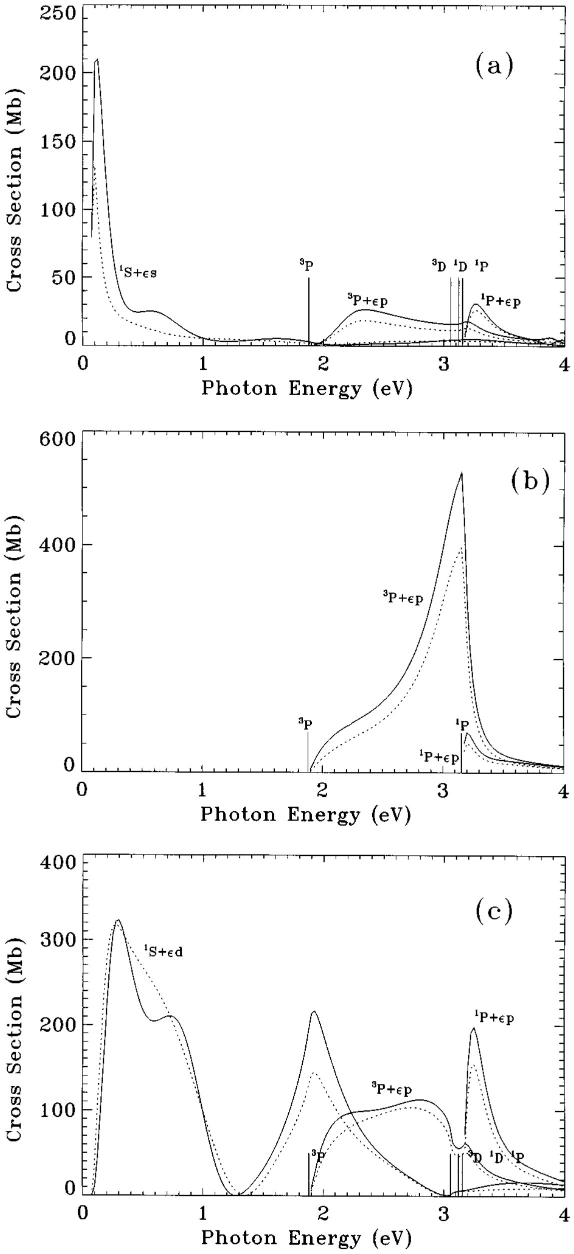

FIG. 6. The main contribution of the individual ionization channels to the (a) ^2S partial cross section, (b) ^2P partial cross section, and (c) ^2D partial cross section. Solid lines refer to the length form, dotted lines to the velocity form. The calculated excitation thresholds are indicated by vertical lines.

However, as argued by Fischer and Hansen, a description of the neutral target within this range of accuracy should be sufficient because the photodetachment cross section is not sizably sensitive to the target state but rather to the continuum wave function and that of the extra electron bound to the neutral target. One should therefore hardly expect so large a discrepancy between our results and those of Fischer and Hansen. Another difference between our and their calculations can be seen in the generation of the initial state of the photodetached ion. Due to the inclusion of more numerical basis functions, we can allow the wave function to extend even to the R-matrix boundary. This ensures a relatively accurate description of the very loosely bound state, which is an indispensable requirement for treating photodetachment.

In order to clarify the origin of the structures in the energy dependence of the photodetachment cross section which Fig. 5 refers to, we have extracted from our calculations the contribution of the major ionization channel to the three partial cross sections. The result is shown in Fig. 6. As follows from inspection of Fig. 6(a), there are two weak shape resonances that relate to the ionization channels $(4s4p^3P+\epsilon p)^2S$ and $(4s4p^1P+\epsilon p)^2S$. From Fig. 6(b), it can clearly be seen that the increase of the total cross section at 2.5 eV originates mainly in the contribution of the $(4s4p^3P+\epsilon p)^2P$ ionization channel. The sharp increase of the cross section in Fig. 6(b) is most likely caused by the interaction between the $(4s4p^3P+\epsilon p)^2P$ and the $(4s4p^1P+\epsilon p)^2P$ channels. Channel contributions to the ^2D partial cross section are displayed in Fig. 6(c). The behavior of the $(4s4p^3P+\epsilon p)^2D$ cross section reflects the channel interaction we referred to in discussing the ^2D partial cross section of Fig. 1. The sharp shape resonance structure of the $(4s4p^1P+\epsilon p)^2D$ channel is also produced by our calculation, which was used by Walter and Peterson [29] in their measurement of electron affinity of Ca atoms.

In summary, we have carried out calculations on electron scattering by Ca atoms and photodetachment of Ca^- ions by using the R-matrix method. Interactions between certain channels are found to be important to explain the essential features of the experimental data. The results of our calculation agree reasonably well with the experiments. As for the photodetachment cross section there is a quantitative discrepancy between our results and those obtained from other theories. In order to resolve the considerable differences between the existing theories, further independent calculations and experiments at an improved accuracy level appear to be very desirable.

ACKNOWLEDGMENTS

We would like to thank Professor I. I. Fabrikant for furnishing us with very detailed tables on his results. This work was supported in part by the National Natural Science Foundation of China and also by the Ministry of Education and Research (BMBF) of the Federal Republic of Germany.

---

[1] D. J. Pegg, J. S. Thompson, R. N. Compton, and G. D. Alton, Phys. Rev. Lett. **59**, 2267 (1987).
[2] C. F. Fischer, J. B. Lagowski, and S. H. Vosko, Phys. Rev. Lett. **59**, 2263 (1987); C. F. Fischer, Phys. Rev. A **39**, 963 (1989).
[3] L. Kim and C. H. Greene, J. Phys. B **22**, L175 (1989).
[4] W. R. Johnson, J. Sapirstein, and S. A. Blundell, J. Phys. B **22**, 2341 (1989).
[5] J. Yuan and Z. Zhang, J. Phys. B **22**, 2751 (1989); Phys. Rev. A **42**, 5363 (1990); J. Yuan, *ibid.* **52**, 4647 (1995).

[6] V. A. Dzuba, V. V. Flambaum, and O. P. Sushkov, Phys. Rev. A **44**, 4224 (1991).
[7] G. F. Gribakin, B. B. Gul'tsev, V. K. Ivanov, M. Ya Kuchiev, and A. R. Trancic, Phys. Lett. A **164**, 73 (1992).
[8] R. Semytkowski and J. E. Sienkiewicz, Phys. Rev. A **50**, 4007 (1994).
[9] G. F. Gribakin, B. V. Gul'tsev, V. K. Ivanov, and M. Ya Kuchiev, J. Phys. B **23**, 4505 (1990).
[10] C. F. Fischer and J. E. Hansen, Phys. Rev. A **44**, 1559 (1991).
[11] I. I. Fabrikant, *Atomniye Protsessi* (Zinatne, Riga, 1975), p. 80, (in Russian).
[12] M. Ya Amusia, V. A. Sosnivker, N. A. Cherepkov, and L. V. Chernysheva, Zh. Tekh. Fiz. **55**, 2304 (1985) [Sov. Phys. Tech. Phys. **30**, 1369 (1985)]; M. Ya Amusia and V. A. Sosnivker, *ibid.* **59**, 28 (1989) [**34**, 270 (1989)].
[13] N. I. Romanyuk, O. B. Shpenik, and I. P. Zapesochyi, Pis'ma Zh. Éksp. Teor. Fiz. **32**, 472 (1980) [JETP Lett. **32**, 452 (1980)].
[14] N. I. Romanyuk, O. B. Shpenik, F. F. Papp, I. V. Chernysheva, I. A. Mandi, V. A. Kelemen, E. P. Sabad, and E. Yu. Remeta, Ukr. Fiz. Zh. **37**, 1639 (1992).
[15] A. R. Johnston, G. A. Gallup, and P. D. Burrow, Phys. Rev. A **40**, 4770 (1989).
[16] E. Heinicke, H. J. Kaiser, R. Rackwits, and D. Feldmann, Phys. Lett. A **50**, 265 (1974).
[17] K. A. Berrington, P. G. Burke, M. LeDourneaf, W. D. Robb, K. T. Taylor, and Vo KyLan, Comput. Phys. Commun. **14**, 367 (1978).
[18] P. G. Burke, A. Hibbert, and W. D. Robb, J. Phys. B **4**, 153 (1971).
[19] E. Clementi and C. Roetti, At. Data Nucl. Data Tables **14**, 177 (1974).
[20] A. Hibbert, Comput. Phys. Commun. **9**, 141 (1975).
[21] H. A. Kurtz and K. D. Jordan, J. Phys. B **14**, 4361 (1981).
[22] I. I. Fabrikant, J. Phys. B **26**, 2533 (1993).
[23] C. Greene, U. Fano, and G. Strinati, Phys. Rev. A **19**, 1485 (1979); S. Watanabe and C. H. Greene, *ibid.* **22**, 158 (1980).
[24] V. V. Petrunin, H. H. Andersen, P. Balling, and T. Andersen, Phys. Rev. Lett. **76**, 744 (1996).
[25] D. Hanstorp, P. Derynck, W. G. Graham, and J. R. Peterson, Phys. Rev. Lett. **63**, 368 (1989).
[26] D. Sundholm and J. Olsen, Chem. Phys. Lett. **217**, 451 (1994).
[27] Hugo W. van der Hart, C. Laughlin, and J. E. Hansen, Phys. Rev. Lett. **71**, 1506 (1993).
[28] Sten Salomonson, H. Warston, and I. Lindgren, Phys. Rev. Lett. **76**, 3092 (1996).
[29] C. W. Walter and J. R. Peterson, Phys. Rev. Lett. **68**, 2281 (1992).